IJE TRANSACTIONS C: Aspects Vol. 25, No. 3, (September 2012) 177-186

Intrnational Journal of Engineering

Journal Homepage: www.ije.ir

Numerical Modeling of an Innovative Bipolar Plate Design Based on the Leaf Venation Patterns for PEM Fuel Cells

F. Arbabi, R. Roshandel*, G. Karimi Moghaddam

Energy Engineering Department, Sharif Energy Research Institute (SERI), Sharif University of Technology, P.O. Box 11365-9567, Tehran-Iran, Tel: +98 (21) 6616 6127, Fax: +98 (21) 6616 6102

ARTICLE INFO

Article history:
Received 6 February 2011
Accepted in revised form 14 June 2012

Keywords:
Fuel Cells
Bipolar Plate
Flow Field Design
Computational Modeling
Leaf Venation Pattern

ABSTRACT

Flow channel design on bipolar plates has a direct effect on Proton Exchange Membrane (PEM) fuel cell performance. It has been found out that the flow field design has a deterministic role on the mass transport and water management, and therefore on the achieved power in PEM Fuel cells. This study concentrates on improvements in the fuel cell performance through optimization of channel dimensions and configuration. To find an optimized state, a two dimensional numerical model of the flow distribution based on the Navier-Stokes equations and by use of an individual computer code is presented. The simulated results showed a very good agreement with the experimental results obtained in previous works. Finally, numerical simulation has been conducted to investigate the advantages of a newly proposed pattern with inspiration from plant leaves. The main design criteria are focused on less pressure drop and more uniform pressure and velocity distributions throughout the flow channels. It was found that both velocity and pressure fields are much more homogeneous in the new channel design; therefore, it is expected to produce a more uniform dispersal of reactants over the GDL and the catalyst layer, which in turn causes the efficiency to enhance.

doi: *10.5829/idosi.ije.2012.25.03c.01*

1. INTRODUCTION

Proton exchange membrane fuel cells can provide potential advantages of clean and renewable energy conversion systems for automotive, portable applications and stationary power generation equipment. Energy demand worldwide encourages scientists to look for the new energy sources, preferably green and renewable ones. As a matter of fact, fuel cells technology is one of the most reliable sources to solve growing energy demand on earth. In hydrogen fuel cells, water is the single byproduct generated by hydrogen chemical reaction with oxygen. Because of its high efficiency, low-temperature, high achieved power density and short startup time, PEM fuel cells have found a special place amongst other types of fuel cells and have rapidly passed the stages of industrialization. PEM fuel cells have been broadly used since the early years of space programs, in submarine vessels, as well as in the automotive industry.

*Corresponding Author Email: *Roshandel@ sharif.edu* (R. Roshandel)

Bipolar plates are one of the most important and effective elements on efficiency and power density gains of fuel cells. These components supply fuel and oxidant to the reactive zones, remove reaction products, collect produced current and provide mechanical support for the cells in the stack. More than 60% of the weight and 30% of the total cost of fuel cells stacks is due to bipolar plates [1]. Some of the major challenges for improving the efficiency of fuel cells are improvments in the performance and increasing the reliability and durability of some of the key components such as the membrane electrode assembly (MEA) and the bipolar plates. An effective design of gas flow field, through optimization of the channel dimensions, shape and configuration may results in an enhanced bipolar plate.

There are many open source literatures worked on different aspects of fuel cell technologies, covering a wide range of concepts from dynamic control and heat transfer analysis to water management and material selection [2-17]. Much research work has been carried out to investigate the effect of various flow field patterns on the fuel cell performance [1, 18-29]. For this

purpose, some bipolar plate geometries such as squared spots, interdigitated, serpentine, spirals or even porous carbon and perforated stainless steel designs are typically considered in the open literature. The advantages and disadvantages of various bipolar plate designs are discussed in the reviews by Carrette and Friedrich [18] and Yang et al. [30]. Hontanon et al. [24] studied the gas flow distribution system using a 3D numerical model, concluding that the porous materials could yield better flow distributions and reactant gas utilization in comparison with grooved plates. The flow distribution with a parallel-channel was analyzed using both experimental and numerical simulation techniques by Barreras et al. [20]. Indeed, Lozano et al. [27] studied the fluid dynamic performance in three different bipolar plates using computational modeling and experimental methods. The proposed configurations were a set of parallel diagonal channels, a branching cascade type, and serpentine - parallel channels. Zhou et al. [29] designed a new flow field to find a better flow field due to its extensibility. There are many independent inlets and outlets in their new flow field.

An appropriate bipolar plate design can provide a high contact surface area as well as a homogeneous reactant gas dispersion to obtain more enhanced mass transport rates without increasing the pressure drop. The main criteria to design and fabricate flow fields are as follow:

1. 2. Flow Channel Path Configuration The reactants' moving paths are one of the most important matters in flow field design. Different path configurations are considered to improve the mass transport inside the gas-gas diffusion layer, as well as reaction kinetics in the catalyst layer.

1. 3. Material Selection Alternative materials and manufacturing techniques for bipolar plates need to be investigated. Properties including electrical conductivity, corrosion resistance, ease of manufacturability, high electrical conductivity, and thin and lightweight plates, are the main criteria in the material selection process.

1. 4. Width of the Ribs Between the Channels Minimizing this factor improves mass transport in the gas diffusion layer, generally in the regions adjacent to the ribs. However, the porosity and permeability of the gas diffusion layer may reduce in the regions underneath the ribs due to the packing pressure.

1. 5. Channel Cross-section This aspect affects the flow velocity and pressure loss, which influences water flooding and efficiency.

1. 6. Ratio of Channel to Land Area Minimizing channel to land area also makes electron collection more difficult.

1. 7. Channel Length Long channels will cause more pressure drop in bipolar plates.

The objective of this work is to improve the performance of PEM fuel cells through optimization of dimensions and shape of flow channels. Approach used in this research, is based on the computational fluid dynamic (CFD) investigation of several flow field topologies. In this work, at the first step, the fluid dynamics studies have been conducted with neglecting the effects of electrochemical reaction.

The effects of various channels and lands dimensions in different patterns such as the parallel, one path parallel - serpentine and three path parallel-serpentine flow channels have been simulated. Since the bipolar plates collect produced current and provide mechanical support for MEA, the fraction of the land area to the channel area should be in the adequate range. For design and optimization purposes, a 2D computer code based on the finite volume method using SIMPLE algorithm is developed, founded on the steady Navier–Stokes equations. The outcomes of the numerical simulations showed a very good agreement with the experimental results in previous works. This confirms the validity of the numerical code for studying design parameters without the need of actually fabricating the plates. Furthermore, effects of electrochemical reactions on the pressure and velocity profiles in bipolar plates are investigated in the final step. After comparing the performance of different patterns on the bipolar plates, the idea of using xylem patterns of leaves in nature is presented and analyzed. This pattern is based on drafts, which exist in nature, patterns which have been improved during millions of years of evolution. We can see the simplest example of these patterns in the veins of plants and leaves, as well as the blood distribution system in the body. A sample of leaf venation pattern is exhibited in Figure 1.

In short, our main research highlights in this exploration are as follows:

- Develop a two dimensional model based on the finite volume method,
- Simulate the conventional types of flow field patterns (parallel and two types of serpentine bipolar plates),
- Present a new innovative flow field design based on the existing samples in nature,
- Comparison and evaluation of different flow field types by obtaining their performance and power densities.

Figure 1. Leaf venation flow patterns in the nature

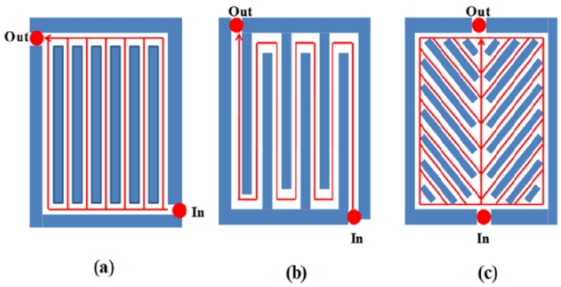

Figure 2. Geometry and configuration of different flow fields (a) parallel flow field (b) serpentine bipolar plate and (c) bio inspired flow field

2. THE PROBLEM UNDER STUDY

Bipolar plates are tools to distribute hydrogen and air on anode or cathode of PEM fuel cells. In short, bipolar plates do three main tasks: (1) supply reactants, (2) remove the reactant products (water) and (3) harvest the electrical current.

Many researchers have focused on design of bipolar plates; we can categorize these designs to three main groups;

2. 1. Parallel Flow Field Reactant gas enters through the header inlet and then enters different interior gas channels and flows out from the header outlet.

2. 2. Serpentine Flow Field Only one flow path exists in serpentine flow fields, so liquid water is forced to exit the channel.

2. 3. Interdigited Flow Field In this pattern, the reactant gases forced to flow through the gas diffusion layer.

In this paper, the idea of using Bio Inspired (BI) flow field based on the leaf venation is presented. Reactant gases enter through the middle, distribute across the symmetric diagonal parallel channels and exit through the middle of the cell. The distance between channels decreases while the flow approaches to outlet to provide more homogenous velocity and species distribution throughout the cell. In this work, we consider interdigited design as a future work, while the other flow fields are studied and compared. Parallel, serpentine and BI flow field configurations are schematically depicted in Figure 2.

Fluid flow analysis in different topologies of flow channels are considered in this study. The following assumptions were used in developing the models as used in similar works [20, 27, 29]

(1) Steady state conditions exist in the single cell. The effect of gravity was also neglected.
(2) Reactant gases are incompressible and Isothermal conditions exist in the cell domain [9].
(3) Based on Reynolds number (Re=68) [20, 27] the flow in the fuel cell is laminar and all the transport equations were formulated for laminar behavior.
(4) The volume of by-product liquid H_2O was assumed negligible in the domain. Hence, working fluid has been considered as the single component H_2 gas at constant temperature [20].

3. Numerical Simulation and Governing Equations

For design and optimization, based on the steady Navier–Stokes equations, a two dimensional CFD code has been developed for different flow-field patterns. In the second step, Fick's law, Butler-Volmer equation and species transport equations is used to describe the current and species distribution in the flow field. The numerical analysis has been performed for an X–Y plane. To obtain the computational code, a finite volume method has been preferred over other methods including finite element approaches, to discretize the mathematical equations [31]. Finite difference methods usually have a non-conservative foundation and may lead to a divergent result for velocity-pressure coupled problems like this. This coupling is numerically implemented using SIMPLE algorithm [32]. A staggered grid has been employed to the Cartesian coordinate system to improve the velocity–pressure coupling quality. Finally, a gradient-conjugate iterative technique has been used to solve the equation system [31]. The numerical modeling algorithm, which is used in this study, is presented in Figure 3. The equation of mass conservation for the reactant gas in fuel cell channels and gas diffusion layer could be written as follows:

$$\nabla \left(\varepsilon \rho \vec{u} \right) = S_m \quad (1)$$

where $\vec{u}$ denotes the velocity vector of the fluid flow, ρ is the gas mixture density and ε is the porosity of the porous electrode. The mixture density is determined using the ideal gas mixing law,

$$\rho_{mix} = \frac{P_{op}}{RT\sum(\frac{X_i}{M_i})} \quad (2)$$

where P_{op}, R, T, X_i and M_i indicate the operating pressure, universal gas constant, operating temperature, mole fraction of chemical species i and the molecular weight of species i, respectively. The mass fraction is related to mole fraction by

$$Y_i = \frac{X_i M_i}{\sum X_i M_i} \quad (3)$$

The summation of all mass fractions is equal to unity

$$\sum Y_i = 1 \quad (4)$$

This can be used to determine the mass fraction (and also mole fraction) of the third component on both sides (Nitrogen at cathode and Carbone dioxide at anode). Momentum equations in the domain (Navier- Stokes equations) are given by

$$\nabla(\varepsilon\rho\vec{u}\vec{u}) = -\varepsilon\nabla p + \nabla(\varepsilon\mu\nabla\vec{u}) + S_u + S_{mom} \quad (5)$$

Here p is the pressure and μ is the dynamic viscosity. S_u in the above equation is due to presence of porous media and can be stated as follows:

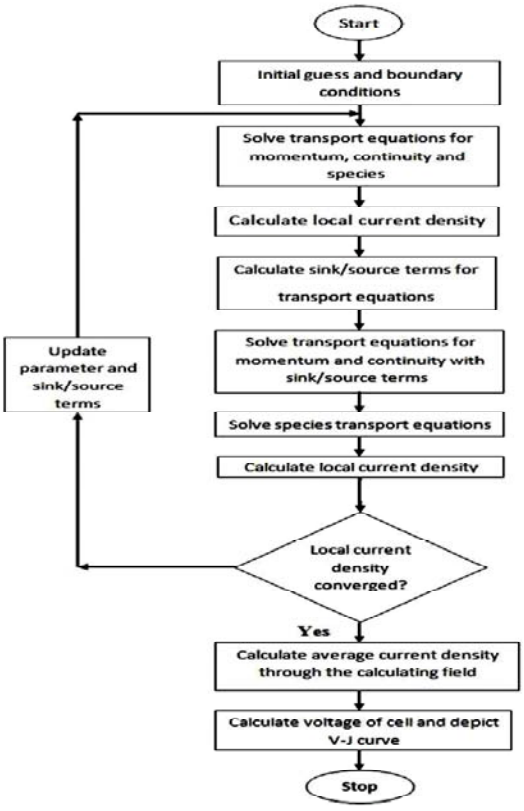

Figure 3. Numerical algorithm to solve the governing equations.

$$S_u = -(\frac{\mu}{k})\varepsilon\vec{u} \quad (6)$$

k is the GDL permeability. S_{mom} is the momentum source term due to the mass generation/consumption in x, y, z directions on account of the electrochemical reactions

$$S_{mom} = S_m\vec{u} \quad (7)$$

3. 1. Chemical Reactions Species transport equation is governed by

$$\nabla(\rho\varepsilon\vec{u}Y_i) = \nabla\left(\rho D_i^{eff}\varepsilon\nabla Y_i\right) + S_i \quad (8)$$

here Y_i is the mass fraction of the *i* th species and D_i^{eff} denotes the effective diffusion coefficient, that is

$$D_i^{eff} = \varepsilon^{1.5} D_i \quad (9)$$

The source term in Equation (8) can be introduced as follows:

for the anode side

$$S_{H_2} = -(\frac{j_a}{2F})M_H \quad (10)$$

and for the cathode side

$$S_{O_2} = -(\frac{j_c}{4F})M_O \quad (11)$$

$$S_{H_2O,react} = (\frac{j_c}{2F})M_{H_2O} \quad (12)$$

In addition to the water creation in the catalyst layer, the water might travel between the anode and cathode. This water transfer can be due to three effects; electro-osmotic drag, which is because of the potential difference in the charge carrier, back-diffusion due to the different water concentrations in anode and cathode and water transfer caused by the pressure difference in anode and cathode. To consider the effect of these mechanisms, we use the correlated equation observing the relation of these effects, current density and cathode potential stated by Sun et al. [33] which is based on the previous experimental work done by Choi et al. [8]

$$\alpha_w = 46 \times NCO^2 - 31.25 \times NCO + 57 \quad (0.25V \le NCO \le 0.35V) \quad (13)$$

$$\alpha_w = 0.3 \quad (0.35V < NCO)$$

$$\alpha_w = 1 \quad (NCO < 0.25V)$$

NCO is the nominal cathode overpotential, which considers the influence of cathode activation overpotential and Ohmic losses due to electron resistance in the catalyst layer and the GDL, as well as the effect of proton resistance in the catalyst layer. The overall consequence of the water transfer across the membrane is outlined by

$$S_{H_2O,flux} = -\frac{2\alpha_w j_c}{2F} M_{H_2O} \quad (14)$$

Therefore, the total source term of water can be stated as

$$S_{H_2O} = S_{H_2O,flux} + S_{H_2O,react} \quad (15)$$

Our focus in this research is on the cathode side; however, we can use the same equations for fluid flow and the stated above equation for species transport in the anode side as well. In Equations (1 and 7) the S_m source term can be written as follows:

for the anode side

$$S_m = S_{H_2} + S_{H_2O} \quad (16)$$

and for the cathode side

$$S_m = S_{O_2} + S_{H_2O} \quad (17)$$

Both generation or consumption of chemical species and the creation of electric current take place in the thin catalyst layer where electrochemical reactions happen. The transfer current, j, is represented by the famous Butler-Volmer equation in anode and cathode [21]

$$j_a = j_{0,a}^{ref}\left(\frac{c_{H_2}}{c_{H_2,ref}}\right)^{0.5}\left\{\exp\left(\frac{\alpha_a F\eta_a}{RT}\right) - \exp\left(-\frac{\alpha_c F\eta_a}{RT}\right)\right\} \quad (18)$$

$$j_c = j_{0,c}^{ref}\left(\frac{c_{O_2}}{c_{O_2,ref}}\right)^{1}\left\{\exp\left(\frac{\alpha_a F\eta_c}{RT}\right) - \exp\left(-\frac{\alpha_c F\eta_c}{RT}\right)\right\} \quad (19)$$

where $j_{0,a}^{ref}$ and $j_{0,c}^{ref}$ are the reference exchange current densities, η_a and η_c, the activation overpotentials, c_{H_2} and c_{O_2} are the molar concentrations and α_a and α_c the transfer coefficients at the anode side and cathode side, respectively.

The fuel cell voltage is given by F. Barbir [34]

$$E = E_0 - \Delta V_{act} - \Delta V_{conc} - \Delta V_{ohm} \quad (20)$$

where ΔV_{act} is the activation loss, ΔV_{conc} is the voltage loss due to concentration polarization and ΔV_{ohm} is the Ohmic loss which occurs because of resistance to the flow of ions in the electrolyte and resistance to the flow of electrons across the electrically conductive fuel cell ingredients. E_0 is the thermodynamic open circuit potential which is related to pressure and temperature and can be calculated by Nernst law [21]

$$E_0 = 1.229 - 0.85\times10^{-3}(T - 298.15) + 4.3085\times10^{-5}\,T\left[\ln(p_{H_2}) + \frac{1}{2}\ln(p_{O_2})\right] \quad (21)$$

where T is expressed in Kelvin, and p_{H_2}, and p_{O_2} are expressed in atmosphere in this equation. This is noticeable that all the above equations are reliable for both channel and gas diffusion layer, bearing in mind that the porosity in the flow channel should be considered equal to unity, and the permeability should be considered as infinity.

Finally, the pressure coefficient C_p is the ratio between pressure-difference at inlet pressure to the fluid inlet kinetic energy used as the index of uniformity of pressure distribution in the computational domain;

$$C_p = \frac{\Sigma\left(P_{in}^{*} - P^{*}(i,j)\right)}{N} \quad (22)$$

where P_{in}* is dimensionless inlet pressure, P*(i,j) dimensionless local pressure in each node and N the number of nodes in computational domain. Basic parameters used in the model are given in Table 1.

TABLE 1. Basic parameters

Parameter	Value	Source
Number of the ribs	17	[20]
Height of the plate, H (m)	0.07	[20]
Operating temperature, T (K)	353	[20]
Density of H_2, ρ (kg m^{-3})	0.0674	[20]
Absolute viscosity, μ (Pa.s)	1.05×10^{-5}	[20]
Reynolds number, Re	68	[20]
Reference concentration of H_2, C_{ref} (mol m^{-3})	0.33	[21]
Reference current density for anode electrode, $j^{ref}_{0,a}$ (A m^{-2})	1.5×10^{-2}	[21]
Diffusion coefficient, D_{H2} (m^2 s^{-1})	10^{-4}	[21]
Effective diffusion coefficient, D_{eff} (m^2 s^{-1})	1.49×10^{-5}	[21]
Anodic transfer coefficient, α	0.5	[21]

3. 2. Model Validation For validating the outcomes of the developed code, the experimental velocities obtained by Barreras et al. [20] have been used. In this work, a commercial bipolar plate with a surface area of 50 cm^2 is used. It is formed by 16 central channels 1 mm deep and 3 mm wide, separated by 1mm thick ribs. Two channels in the upper and lower part of the plate with a width of 2 mm surround the whole flow area. The comparison between modeling results and experiments are presented in Figure 4, and as it can be seen, the simulations agree well with experimental data from Barreras et al. [20]. This point confirms the validity of the simulations to study design variations without the need of actually fabricating the plates.

4. ERROR ANALYSIS

To investigate the effects of the discretization on the numerical model, different grid sizes have been studied (70×70,140×140, 210×210). In Figure 5, velocity contours

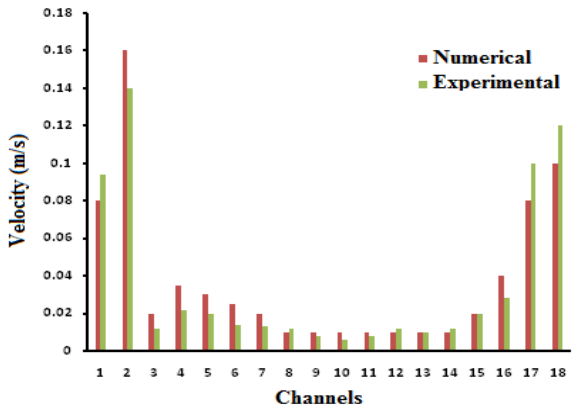

Figure 4. Comparison between the average velocities from the experiments [20] and numerical results

for three different grid generations are shown. It is quite obvious from the figure that the simulated results are well matched. Furtheremore, it can be seen that meshes 140×140 and 210×210 show very close results, which indicate that 140×140 mesh has an accurate enough resolution to simulate with an acceptable precision in our computational domain. The results of the 140×140 mesh converged after about 50,000 iterations with a level of convergence β less than 10^{-6}. The convergence parameter is defined in the following way

$$\text{Diff}\emptyset = \left|\emptyset^{(n)} - \emptyset^{(n-1)}\right| \quad (23)$$

$$\beta = \frac{\sum \text{Diff}\emptyset}{\text{Number of Nodes}} \quad (24)$$

where $\emptyset^{(n)}$ is the velocity and pressure result for iteration number equal to n.

5. RESULTS AND DISCUSSION

Simulation of flow distribution in parallel flow channels is presented in Figure 6. This figure shows a very poor efficiency of velocity and pressure fields in the bipolar plate. Although, most of the reactant gases tend to flow through the side channel and a big amount of the flow tends to move through the first channels. When the fluid concentrates against the second rib, a high-pressure area would form that forces the fluid to flow throughout the first two channels, which causes a more non-homogeneous dispersion. In fact, the fluid velocity along the central channels is so slow and hence it is possible to observe liquid phase formation through the exit in certain cases depending on operational condition and output current density. These results are also confirms by Barreras et al. [20].

To resolve the problem of water accumulation due to low velocity regions, Watkins et al. [35] proposed a continuous fluid-flow channel that applied an inlet at one end and an outlet at the other side and typically followed a serpentine path. In an attempt to tackle the problems with straight flow channels, we simulated serpentine gas flow fields across the plate surface. As shown schematically in Figure 7, a single serpentine flow field forces the reactant flow to traverse the entire of the plate and thereby eliminating areas of stagnant flow. Moreover, the distribution of reactant gases in channels are relatively homogenous, thus the proposed flow field design can improve reactant flow distribution across the electrode surface below the bipolar plate. However, this channel layout results in a relatively long reactant flow path, and therefore, a substantial pressure drop and significant concentration gradients in flow field could be expected as it has been indicated by Xianguo et. al [29]. Figures 8 and 9 show the simulation results for two other types of serpentine flow fields. The simulated patterns ensure proper product removal through the channels and there is no stagnant area formation on the surface of plate. Therefore, it can be more effective for water accumulation problem in low temperature fuel cell applications. As a result, the output power may enhance with these types of flow-field plates. By looking at these figures, it is obvious that multiple serpentine flow-fields reduce the reactant pressure drop in comparison with single serpentine flow fields.

Figure 10 presents pressure and velocity profiles for simulated pattern in the leaf venation inspired flow channels. As it can be seen in this figure, there are very good improvements in velocity and pressure fields in the new pattern; it means that, there are more homogeneous velocity and pressure distributions in the flow field. Most importantly, the pattern shows very low pressure drop. However, there are two land free regions in the lowest corners of the plate and hence the electron transport may be influenced. It is well known that the electron transport is necessary for fuel cell electrochemical reactions. As the ratio of land/channel becomes smaller, Ohmic overpotential will be increased, and the overall fuel cell performance is degraded as well. The next important step in flow field design is to fill the free region by proper additional channels, which are presented in Figure 11. However, in the revised version, total pressure drop has increased. However, in comparison with other conventional patterns, it is still acceptable.

As mentioned before, total pressure drop and reactant concentration uniformity are two main parameters, which have a significant effect on the bipolar plate performance.

Figures 12 and 13 present the comparison of these two parameters in different bipolar plate configurations. It is obvious that BI pattern has less pressure drop as well as more uniform reactant concentration throughout the electrode surface.

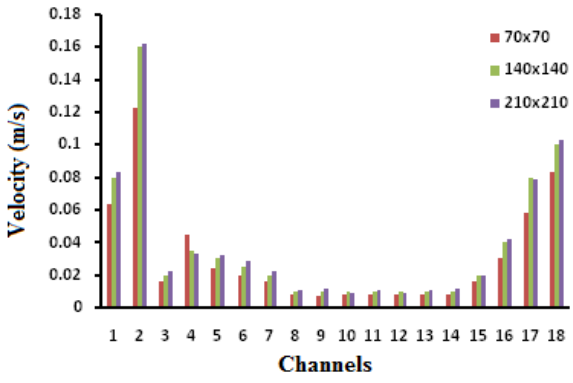

Figure 5. Fluid velocity in the channels for the three different grids sizes

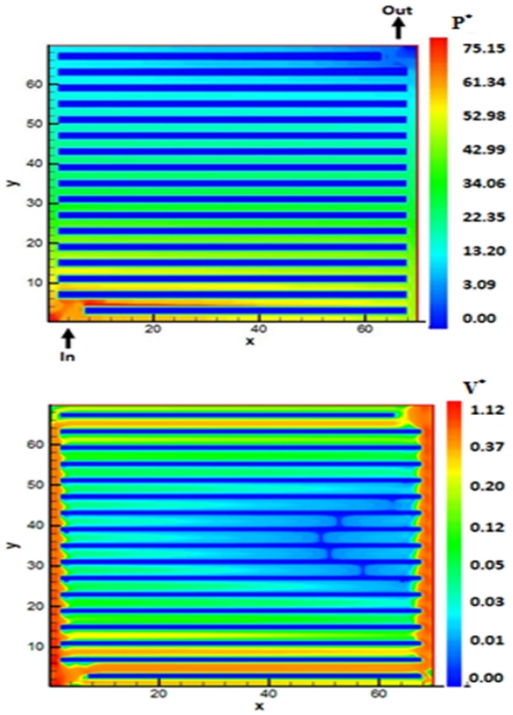

Figure 6. Dimensionless pressure and velocity fields in parallel flow pattern

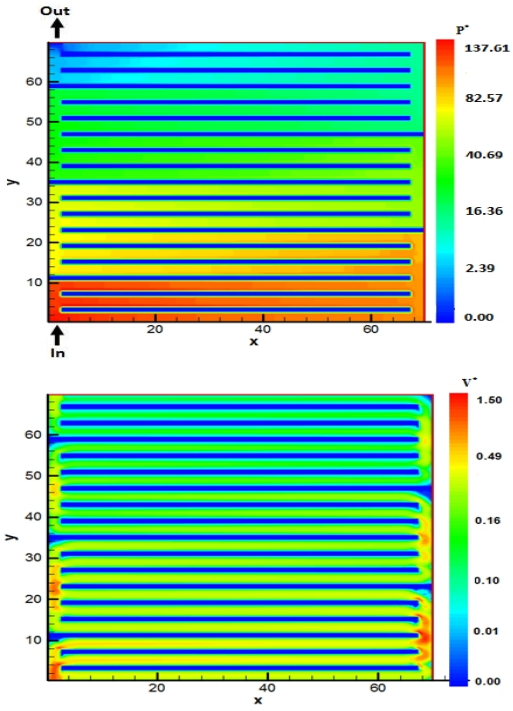

Figure 8. Dimensionless pressure and velocity fields in three-path serpentine flow pattern (Type I)

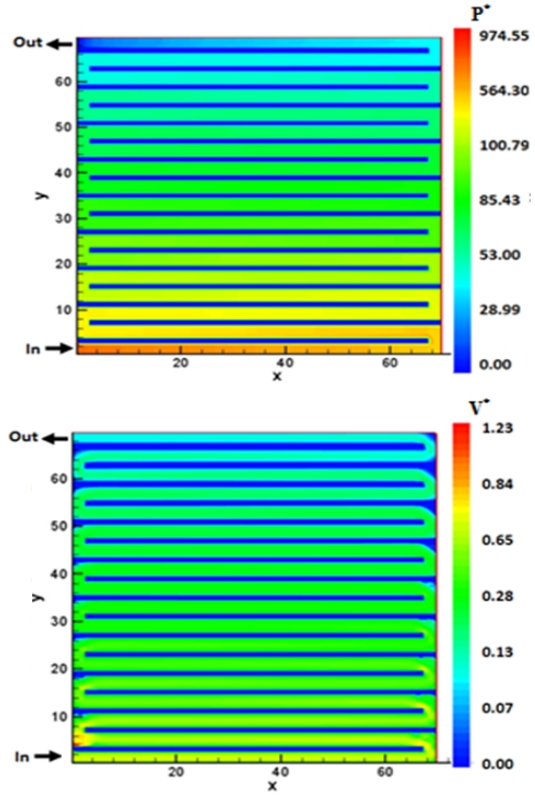

Figure 7. Dimensionless pressure and velocity fields in single serpentine flow pattern

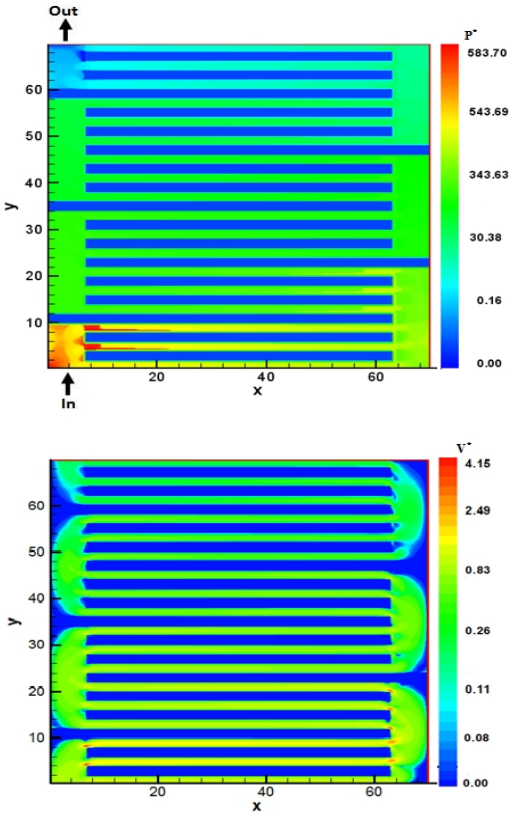

Figure 9. Dimensionless pressure and velocity fields in three-path serpentine flow pattern (Type II)

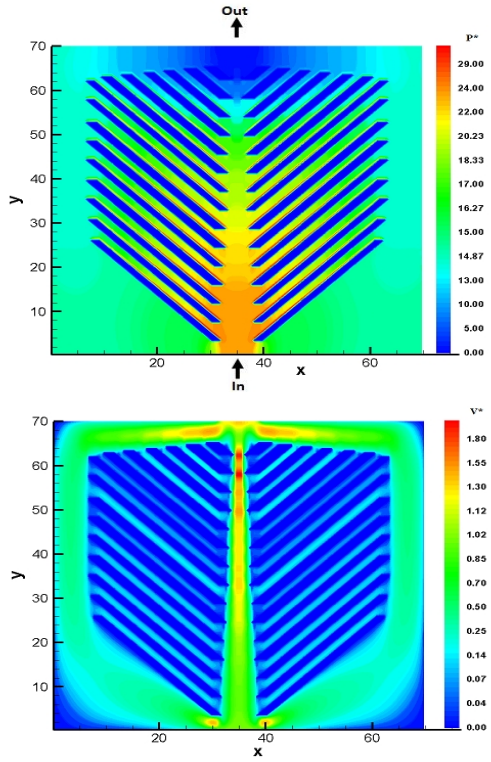

Figure 10. Dimensionless pressure and velocity fields in leaf xylem flow pattern

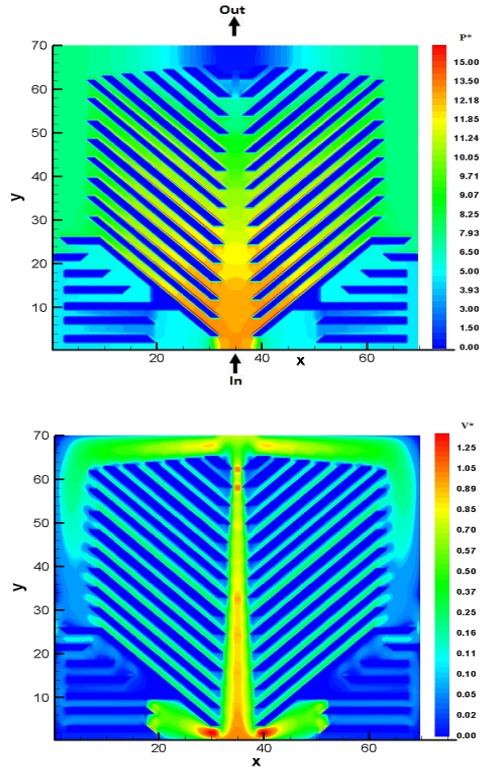

Figure 11. Dimensionless pressure and velocity fields in revised leaf xylem pattern

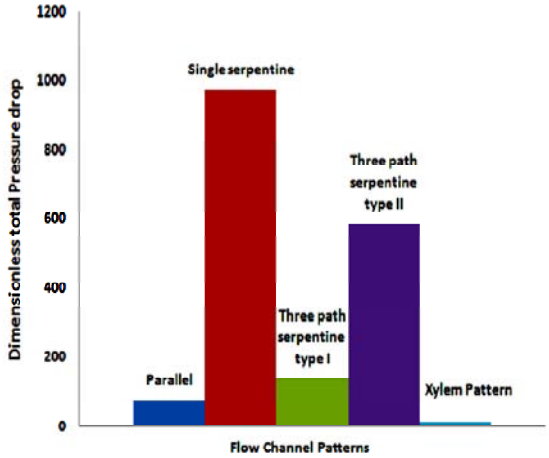

Figure 12. Comparison of total pressure drop in different flow field patterns

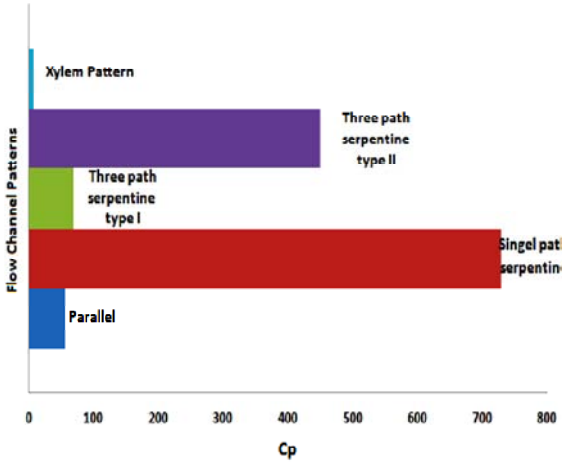

Figure 13. Comparison of pressure uniformity index in different flow field patterns

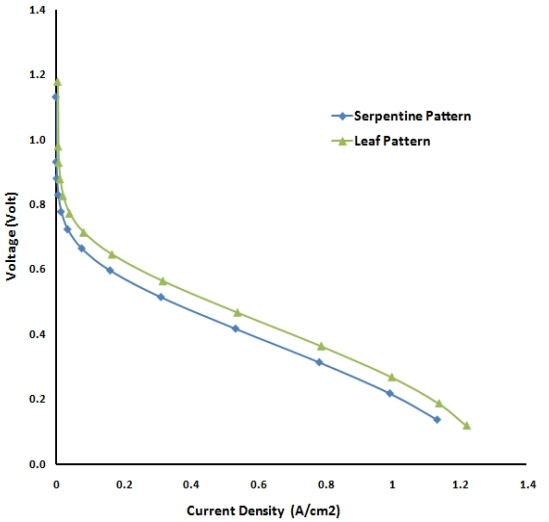

Figure 14. Comparison of polarization curves in two path serpentine and leaf xylem patterns

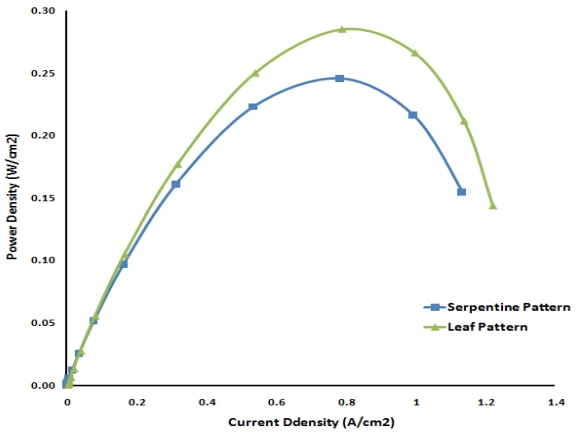

Figure 15. Comparison of power density and current density curves in three-path serpentine and BI patterns

To ensure improvement in fuel cell performance by BI bipolar plate, polarization and power curves for serpentine and BI bipolar plates are compared in Figures 14 and 15,, and as it expected before power gains were increased by the new configuration.

At the end, this is noticeable that this model is not the best bipolar plate that can be designed for a PEMFC; this is just a first step to develop new patterns to improve the efficiency of the fuel cells and increase the achieved energy for future demands.

6. CONCLUSION

Proton exchange membrane (PEM) fuel cell performance is directly related to the flow channel design on bipolar plates. Power gains can be found by varying the type, size, or arrangement of flow channels. This paper presents a two-dimensional, steady state model to investigate different flow channel designs and configurations in bipolar plate. The approach used in this work, is based on CFD investigation of several flow field topologies. After comparison of advantages and disadvantages of conventional bipolar plats design, the idea of using leaf venation patterns is presented and analyzed by a two dimensional numerical model. Simulation results indicate improvement in the fuel cell performance by eliminating the stagnation points in flow field channels. It is found that the patterns with inspiration from leaf venation show appropriate pressure drop and uniform pressure and velocity distribution along the channels. It is also concluded that power density can be improved up to 8% in the new pattern; meanwhile total pressure drop in this pattern is much lower than that in other conventional patterns which leads to improvement in total efficiency of the fuel cell system.

7. REFERENCES

1. Li, X. and Sabir, I., "Review of bipolar plates in PEM fuel cells: Flow-field designs", *International Journal of Hydrogen Energy*, Vol. 30, (2005), 359-371.
2. Baik, K. D. and Kim, M. S., "Characterization of nitrogen gas crossover through the membrane in proton-exchange membrane fuel cells", *International Journal of Hydrogen Energy*, Vol. 36, (2011), 732-739.
3. Bao, C., Ouyang, M. and Yi, B., "Analysis of the water and thermal management in proton exchange membrane fuel cell systems", *International Journal of Hydrogen Energy*, Vol. 31, (2006), 1040-1057.
4. Bao, C., "Analysis of Water Management in Proton Exchange Membrane Fuel Cells", *Tsinghua Science & Technology*, Vol. 11, (2006), 54-64.
5. Bao, C., Ouyang, M. and Yi, B., "Modeling and control of air stream and hydrogen flow with recirculation in a PEM fuel cell system--II. Linear and adaptive nonlinear control", *International Journal of Hydrogen Energy*, Vol. 31, (2006), 1897-1913.
6. Baschuk, J. J. and Li, X., "Modeling of ion and water transport in the polymer electrolyte membrane of PEM fuel cells", *International Journal of Hydrogen Energy*, Vol. 35, (2010), 5095-5103.
7. Chen, S. L., Krishnan, L., Srinivasan, S., Benziger, J. and Bocarsly, A. B., "Ion exchange resin/polystyrene sulfonate composite membranes for PEM fuel cells", *Journal of Membrane Science*, Vol. 243, (2004), 327-333.
8. Choi, K. H., Peck, D. H., Kim C. S., Shin, D. R. and Lee, T. H., "Water transport in polymer membranes for PEMFC", *Journal of Power Sources*, Vol. 86, (2000), 197-201.
9. Debe, M. K., Schmoeckel, A. K., Vernstrom, G. D. and Atanasoski, R., "High voltage stability of nanostructured thin film catalysts for PEM fuel cells", *Journal of Power Sources*, Vol. 161, (2006), 1002-1011.
10. Dokkar, B., Settou, N. E., Imine, O., Saifi, N., Negrou, B. and Nemouchi, Z., "Simulation of species transport and water management in PEM fuel cells", *International Journal of Hydrogen Energy*, Vol. 36, (2011), 4220-4227.
11. Falcão, D. S., Oliveira, V. B., Rangel, C. M., Pinho, C. and Pinto, A. M. F. R., "Water transport through a PEM fuel cell: A one-dimensional model with heat transfer effects", *Chemical Engineering Science*, Vol. 64, (2009), 2216-2225.
12. Gao, F., Blunier, B., Miraoui, A. and El-Moudni, A., "Cell layer level generalized dynamic modeling of a PEMFC stack using VHDL-AMS language", *International Journal of Hydrogen Energy*, Vol. 34, (2009), 5498-5521.
13. Gerard, M., Poirot-Crouvezier J. P., Hissel, D. and Pera M. C., "Oxygen starvation analysis during air feeding faults in PEMFC", *International Journal of Hydrogen Energy*, Vol. 35, (2010), 12295-12307.
14. Hasani-Sadrabadi, M. M., Dashtimoghadam, E., Majedi, F. S., Kabiri, K., Solati-Hashjin M. and Moaddel, H., "Novel nanocomposite proton exchange membranes based on Nafion® and AMPS-modified montmorillonite for fuel cell applications", *Journal of Membrane Science*, Vol. 365, (2010), 286-293.
15. Naterer, G. F., "Fuel channel friction and thermal irreversibilities in a proton exchange membrane fuel cell", *International Communications in Heat and Mass Transfer*, Vol. 33, (2006), 269-277.
16. Van den Oosterkamp, P. F., "Critical issues in heat transfer for fuel cell systems", *Energy Conversion and Management*, Vol. 47, (2006), 3552-3561.
17. Wang, F.-C. and Ko, C.-C., "Multivariable robust PID control for a PEMFC system", *International Journal of Hydrogen Energy*, Vol. 35, (2010), 10437-10445.

18. Carrette, L., Friedrich, K. A. and Stimming, U., "Fuel Cells - Fundamentals and Applications", *Wiley online library*, Vol. 1, (2001), 5-39.
19. Roshandel, R., Arbabi, F. and Karimi Moghaddam, G., "Simulation of an innovative flow-field design based on a bio inspired pattern for PEM fuel cells", *Renewable Energy*, Vol. 41, (2012), 86-95.
20. Barreras, F., Lozano, A., Valino, L., Marın, C. and Pascau, A., "Flow distribution in a bipolar plate of a proton exchange membrane fuel cell: experiments and numerical simulation studies", *Journal of Power Sources*, Vol. 144, (2005), 54-66.
21. Berning, T. and Djilali, N., "Three-dimensional computational analysis of transport phenomena in a PEM fuel cell", *Journal of Power Sources*, Vol. 106, (2002), 284-294.
22. Chen, F., Wen, Y.-Z., Chu, H.-S., Yan, W.-M. and Soong, Ch.-Y., "Convenient two-dimensional model for design of fuel channels for proton exchange membrane fuel cells," *Journal of Power Sources*, Vol. 128, (2004), 125-134.
23. Ferng, Y. M. and Su, A., "A three-dimensional full-cell CFD model used to investigate the effects of different flow channel designs on PEMFC performance", *International Journal of Hydrogen Energy*, Vol. 32, (2007), 4466-4476.
24. Hontañón, E., Escudero, M. J., Bautista, C., Garcıa-Ybarra, P. L. and Daza, L., "Optimisation of flow-field in polymer electrolyte membrane fuel cells using computational fluid dynamics techniques", *Journal of Power Sources*, Vol. 86, (2000), 363-368.
25. Hu, M., Gu, A., Wang, M., Zhu, X. and Yu, L., "Three dimensional, two phase flow mathematical model for PEM fuel cell: Part I. Model development", *Energy Conversion and Management*, Vol. 45, (2004), 1861-1882.
26. Liu, X. and Zhi Wen, G. L., "Three-dimensional two-phase flow model of proton exchange membrane fuel cell with parallel gas distributors", *Journal of Power Sources*, Vol. 195, (2009), 2764-2773.
27. Lozano, A., Luis, V. G., Felix, B. T. and Rado, M. O., "Fluid dynamics performance of different bipolar plates: Part II. Flow through the diffusion layer", *Journal of Power Sources*, Vol. 179, (2008), 711-722.
28. Miansari, M., Sedighi, K., Amidpour M., Alizadeh, E. and Miansari, Mo., "Experimental and thermodynamic approach on proton exchange membrane fuel cell performance", *Journal of Power Sources*, Vol. 190, (2009), 356-361.
29. Zhou, X., Ouyang, Wenze., Liu, C., Lu, T., Xing, W. and An, L., "A new flow field and its two-dimension model for polymer electrolyte membrane fuel cells (PEMFCs)", *Journal of Power Sources*, Vol. 158, (2006), 1209-1221.
30. Yang, C., Costamagna, P., Srinivasan, S., Benziger, J., Bocarsly, A. B., "Approaches and technical challenges to high temperature operation of proton exchange membrane fuel cells", *Journal of Power Sources*, Vol. 103, (2001), 1-9.
31. Ferziger, J. H. and Peric, M., "Computational Methods for Fluid Dynamics", 2 ed. Berlin: Springer-Verlag, 1999.
32. Patankar, S. V., "Numerical HeatTransfer and Fluid Flow", New York: Hemisphere Publishing Corporation, 1980.
33. Sun, W., Peppley, B. A. and Karan, K., "An improved two-dimensional agglomerate cathode model to study the influence of catalyst layer structural parameters", *Electrochimica Acta*, Vol. 50, (2005), 3359-3374.
34. Barbir, F., "PEM Fuel Cells: Theory and Practice", San Diego: Academic Press, 2005.
35. Watkins, D. S. D., Kenneth, W. and Epp, D. G., "Novel fuel cell fluid flow field plate", US Patent, 1991.

Numerical Modeling of an Innovative Bipolar Plate Design Based on the Leaf Venation Patterns for PEM Fuel Cells

F. Arbabi, R. Roshandel, G. Karimi Moghaddam

Energy Engineering Department, Sharif Energy Research Institute (SERI), Sharif University of Technology, P.O. Box 11365-9567, Tehran-Iran, Tel: +98 (21) 6616 6127, Fax: +98 (21) 6616 6102

ARTICLE INFO

Article history:
Received 6 February 2011
Accepted in revised form 14 June 2012

Keywords:
Fuel Cells
Bipolar Plate
Flow Field Design
Computational Modeling
Leaf Venation Pattern

چکیده

عملکرد پیل‌های سوختی غشاء پلیمری تبادل پروتونی مستقیماً به طراحی کانال‌های جریان و صفحات دو قطبی مرتبط است. توان به‌دست آمده بسته به نوع، اندازه یا ترتیب قرارگیری کانال‌ها می‌تواند متغیر باشد. مشخص شده است که طراحی میدان جریان نقشی تعیین کننده روی انتقال جرم و مدیریت آب در پیل‌های سوختی غشاء تبادل پروتونی پلیمری دارد. این تحقیق روی بهبود عملکرد پیل سوختی از طریق بهینه سازی اندازه و ترتیب کانال‌ها تمرکز دارد. برای پیدا کردن حالت بهینه، یک مدل عددی دو بعدی از توزیع جریان بر اساس معادلات ناویر- استوکس و با استفاده از یک کد کامپیوتری ارائه شده است. نتایج حاصل از این مدل سازی تطابق خوبی با نتایج تجربی به‌دست آمده در کارهای قبلی از خود نشان داد. در نهایت، از شبیه سازی عددی برای بررسی مزایای یک طرح تازه، که الهام گرفته از برگ‌های گیاهان می‌باشد استفاده شد. این طراحی باهدف یافتن افت فشار کمتر و توزیع فشار و سرعت همگون‌تر در کانال‌های جریان بوده است. مشخص شد که در طراحی جدید میدان‌های سرعت و فشار بسیار همگنتر می‌باشند، بنابرین، انتظار می‌رود که توزیع واکنش‌گرها روی سطح لایه نفوذ گازی و لایه کاتالیستی بهتر صورت گیرد، که در نهایت باعث بالا رفتن راندمان می‌شود.

doi: *10.5829/idosi.ije.2012.25.03c.01*